Genetics inMedicine | BRIEF REPORT

Official journal of the American College of Medical Genetics and Genomics

Open

Genome-wide multilocus imprinting disturbance analysis in Temple syndrome and Kagami-Ogata syndrome

Masayo Kagami, MD, PhD[1], Keiko Matsubara, MD, PhD[1], Kazuhiko Nakabayashi, PhD[2], Akie Nakamura, MD, PhD[1], Shinichiro Sano, MD, PhD[1], Kohji Okamura, PhD[3], Kenichiro Hata, MD, PhD[2], Maki Fukami, MD, PhD[1] and Tsutomu Ogata, MD, PhD[1,4]

Purpose: Recent studies have identified multilocus imprinting disturbances (MLIDs) in a subset of patients with imprinting diseases (IDs) caused by epimutations. We examined MLIDs in patients with Temple syndrome (TS14) and Kagami-Ogata syndrome (KOS14).

Methods: We studied four TS14 patients (patients 1–4) and five KOS14 patients (patients 5–9) with epimutations. We performed HumanMethylation450 BeadChip (HM450k) analysis for 43 differentially methylated regions (DMRs) (753 CpG sites) and pyrosequencing for 12 DMRs (62 CpG sites) using leukocyte genomic DNA (Leu-gDNA) of patients 1–9, and performed HM450k analysis for 43 DMRs (a slightly different set of 753 CpG sites) using buccal cell gDNA (Buc-gDNA) of patients 1, 3, and 4. We also performed mutation analysis for six causative and candidate genes for MLIDs and quantitative expression analysis using immortalized lymphocytes in MLID-positive patients.

Results: Methylation analysis showed hypermethylated *ZDBF2*-DMR and *ZNF597*/*NAA60*-DMR, hypomethylated *ZNF597*-DMR in both Leu-gDNA and Buc-gDNA, and hypomethylated *PPIEL*-DMR in Buc-gDNA of patient 1, and hypermethylated *GNAS-A/B*-DMR in Leu-gDNA of patient 3. No mutations were detected in the six genes for MLIDs. Expression patterns of *ZDBF2*, *ZNF597*, and *GNAS-A/B* were consistent with the identified MLIDs.

Conclusion: This study indicates the presence of MLIDs in TS14 patients but not in KOS14 patients.

Genet Med advance online publication 15 September 2016

Key Words: epimutation; imprinting; Kagami-Ogata syndrome; multilocus imprinting disturbance; Temple syndrome

INTRODUCTION

The human chromosome 14q32.2 imprinted region harbors paternally and maternally expressed genes, together with the germ line–derived primary *DLK1-MEG3* intergenic differentially methylated region (IG-DMR) and the postfertilization-derived secondary *MEG3*-DMR that function as the imprinting control centers in the placenta and the body, respectively.[1] Consistent with this, maternal uniparental disomy 14 (UPD(14)mat) and loss-of-methylation (LOM)-type epimutations and microdeletions affecting the paternally derived imprinted region lead to Temple syndrome (TS14, OMIM 616222), which is associated with pre- and postnatal growth deficiency, hypotonia, small hands, and precocious puberty.[2] Similarly, paternal uniparental disomy 14 (UPD(14)pat) and gain-of-methylation (GOM)-type epimutations and microdeletions involving the maternally inherited imprinted region result in Kagami-Ogata syndrome (KOS14, OMIM 608149), which is characterized by unique facial features; a small, bell-shaped thorax with a coat-hanger appearance of the ribs; abdominal-wall defects; placentomegaly; and polyhydramnios.[1]

Recent studies have identified multilocus imprinting disturbances (MLIDs) in a subset of patients with imprinting diseases (IDs) caused by epimutations.[3] Indeed, although the frequency of MLIDs is variable among studies, MLIDs have been detected in approximately 50% of patients with transient neonatal diabetes mellitus caused by LOM of the *PLAGL1*-DMR, approximately 12% of patients with Beckwith-Wiedemann syndrome caused by LOM of the *Kv*-DMR or GOM of the *H19*-DMR, 8–10% of patients with Silver-Russell syndrome (SRS) caused by LOM of the *H19*-DMR, and 8–10% of patients with pseudohypoparathyroidism type 1b caused by LOM of the *GNAS-A/B*-DMR, as well as in a single patient with Angelman syndrome caused by LOM of the *SNRPN*-DMR.[3] In addition, although ID-related DMRs have usually been examined to detect MLIDs by conventional methylation analyses including pyrosequencing, genome-wide MLID analysis has become possible by array-based methods.[4] The underlying factors for the MLIDs remain to be clarified in most patients, but the causative genes for MLIDs (*ZFP57*, *NLRP2*, and *NLRP5*), as well as candidate genes for MLIDs (*NLRP7*, *KHDC3L*, and *TRIM28*), have been identified in a few patients with MLIDs.[4,5]

[1]Department of Molecular Endocrinology, National Research Institute for Child Health and Development, Tokyo, Japan; [2]Department of Maternal-Fetal Biology, National Research Institute for Child Health and Development, Tokyo, Japan; [3]Department of Systems BioMedicine, National Research Institute for Child Health and Development, Tokyo, Japan; [4]Department of Pediatrics, Hamamatsu University School of Medicine, Hamamatsu, Japan. Correspondence: Masayo Kagami (kagami-ms@ncchd.go.jp) Or Tsutomu Ogata (tomogata@hama-med.ac.jp)

Submitted 28 March 2016; accepted 12 July 2016; advance online publication 15 September 2016. doi:10.1038/gim.2016.123

MLIDs have been poorly studied in patients with TS14 and KOS14, primarily because of their rarity. To our knowledge, TS14 has been identified in 58 patients, including 10 patients with epimutations of the IG-DMR and the *MEG3*-DMR, and KOS14 has been identified in 57 patients, including 7 patients with epimutations of the two DMRs.[1,2,6–9] Thus, we examined MLIDs in TS14 and KOS14 caused by epimutations.

MATERIALS AND METHODS

Ethical approval

This study was approved by the Institutional Review Board Committee at the National Center for Child Health and Development and was performed after obtaining written informed consent to publish the clinical and molecular information.

Patients

This study consisted of four TS14 patients with LOM-type epimutations (patients 1–4) and five KOS14 patients with GOM-type epimutations (patients 5–9) (**Table 1**). LOMs/GOMs were confirmed by the conventional methylation analysis for IG-DMR and *MEG3*-DMR using leukocyte genomic DNA (Leu-gDNA). UPD(14)mat/pat was ruled out by microsatellite analysis using parental Leu-gDNA, and microdeletions were excluded by fluorescence in situ hybridization analysis of the two DMRs and a custom-built array comparative genomic hybridization analysis for the 14q32.2 imprinted region.[1,10]

Detailed phenotypes are shown in **Supplementary Tables S1 and S2** online. In brief, patient 1 exhibited Prader-Willi syndrome (PWS)-like phenotype in the absence of GOM at the *SNRPN*-DMR, and patients 2–4 manifested SRS-compatible phenotype in the absence of LOM at the *H19*-DMR and UPD(7)mat. Prenatal growth failure was absent from patient 1 and present in patients 2–4, whereas postnatal growth failure was present in patients 1–4. KOS14 patients were identified by the typical phenotype.

Molecular studies

We conducted methylation, mutation, and expression analyses. Detailed methods are described in the **Supplementary Methods** online. In brief, methylation analysis was performed by array-based HumanMethylation450 BeadChip (HM450k) (Illumina, San Diego, CA) analysis for 753 CpG sites on 43 DMRs using Leu-gDNA of patients 1–9 and for a slightly different set of 753 CpG sites on 43 DMRs using epithelial buccal cell gDNA (Buc-gDNA) of patients 1, 3, and 4 (**Supplementary Table S3** online), and by pyrosequencing analysis for 50 CpG sites on nine ID-related DMRs and for 12 CpG sites on three DMRs that were assessed to be abnormally methylated by the HM450k analysis (**Table 1**) using Leu-gDNA of patients 1–9 (for primer information, see **Supplementary Table S4** online). Mutation analysis was performed for the causative and candidate genes for MLIDs (*ZFP57*, *NLRP2*, *NLRP7*, *KHDC3L*, *NLRP5*, and *TRIM28*)[4,5] by whole-exome sequencing using Leu-gDNA of MLID-positive patients and their mothers. Expression analysis was performed by quantitative real-time polymerase chain reaction for imprinted genes regulated by the abnormally methylated DMRs using mRNA samples extracted from immortalized lymphocytes derived from MLID-positive patients. We utilized the nomenclature for DMRs and imprinted genes proposed by the European Network of Human Congenital Imprinting Disorders (http://www.imprinting-disorders.eu/).

RESULTS

Methylation analysis

MLID was identified in patients 1 and 3 with TS14 (**Figure 1a**, **Supplementary Table S3** online, and **Table 1**) (actual methylation levels of each patient and the average ± 3 SD values of control subjects obtained by HM450k analysis are shown in **Supplementary Tables S5 and S6** online). In patient 1, GOM at *ZDBF2*-DMR, LOM at *ZNF597*-DMR, and GOM at *ZNF597*/*NAA60*-DMR were identified by HM450k analysis for Leu-gDNA and Buc-gDNA, with more obvious aberrant methylation patterns in Buc-gDNA than in Leu-gDNA, and by pyrosequencing analysis for Leu-gDNA. In addition, LOM at *PPIEL*-DMR was found only in Buc-gDNA by HM450k analysis. In patient 3, GOM at *GNAS-A/B*-DMR was detected only in Leu-gDNA by HM450k analysis, but not by pyrosequencing analysis.

No other MLID was identified. Although pyrosequencing analysis showed slight GOMs at the #17 CpG site within *PEG10*-DMR in patient 2 and the #27 CpG site within *MEST*-DMR in patient 3 (**Table 1**), other CpG sites within these DMRs were normal. Similarly, although HM450k analysis revealed several abnormally methylated CpG sites (**Figure 1a**, **Supplementary Table S3** online), they accounted for <20% of CpGs within corresponding DMRs.

Of the 11 CpG sites examined by HM450k and pyrosequencing analyses, discordant methylation data were obtained for the #17 CpG site in patient 2 and for the #44 and #45 CpG sites in patient 3. Furthermore, HM450k analysis indicated (i) more severe LOMs at *MEG3*-DMR of Leu-gDNA in patient 1 than in patients 2–4; (ii) more severe LOMs at *MEG3*-DMR in Buc-gDNA than in Leu-gDNA of patients 3 and 4; (iii) invariable GOMs and LOMs at *MEG8*-DMR in TS14 and KOS14 patients, respectively; (iv) normal methylation patterns at *H19*-DMR and *SNRPN*-DMR in Buc-gDNA of patients 1, 3, and 4, as well as in Leu-gDNA of patients 1–9; and (v) hypermethylated *GPR1-AS*-DMR in Leu-gDNA of patients 1–9 and control subjects (**Supplementary Table S5** online).

Mutation analysis

No pathogenic mutation was identified in the six genes of MLID-positive patients 1 and 3 and their mothers.

Expression analysis

Expression analysis revealed significantly increased *ZDBF2* expression and decreased *ZNF597* expressions in patient 1 and significantly decreased *GNAS-A/B* expression in patient 3 (**Figure 1b**).

Table 1 Methylation indices (%) for CpG dinucleotides determined by pyrosequencing analysis for leukocyte genomic DNA samples

		Temple syndrome				Kagami-Ogata syndrome					Controls (n=50)
DMR	**CpG**	**Pt. 1**	**Pt. 2**	**Pt. 3**	**Pt. 4**	**Pt. 5**	**Pt. 6**	**Pt. 7**	**Pt. 8**	**Pt. 9**	**Median (Min–Max)**
TS14-related and KOS14-related DMRs											
IG-DMR	#1	31	34	22	25	91	98	97	93	90	58 (49–68)
(Chr. 14q32.2)	#2	28	33	18	24	95	95	89	70	82	54 (40–62)
	#3	56	57	40	53	90	98	96	100	91	68 (54–78)
	#4	22	25	13	22	88	95	90	77	84	53.5 (43–64)
MEG3-DMR	#5	3	25	3	7	95	96	94	96	93	52 (43–56)
(Chr. 14q32.2)	#6	4	25	3	8	100	99	97	98	97	55 (52–65)
	#7	4	26	4	5	94	95	95	93	91	37 (32–55)
	#8	6	28	6	6	100	99	99	100	96	60 (44–74)
	#9	3	22	2	4	80	84	80	71	71	36 (26–47)
Other imprinting disease-related DMRs											
PLAGL1-DMR	#10[a]	47	51	48	51	43	48	46	48	52	47 (31–52)
(Chr. 6q24.2)	#11	47	47	45	49	44	47	43	45	51	45 (27–51)
	#12	48	45	44	49	52	50	49	51	50	48 (40–56)
	#13	38	37	37	43	42	44	38	40	40	39 (31–47)
	#14	50	47	45	51	51	48	48	54	50	50 (40–58)
	#15	45	45	43	46	52	42	48	49	46	49 (37–55)
	#16	52	50	48	53	57	53	53	55	53	53 (41–58)
PEG10	#17[a]	55	60	53	59	56	59	58	56	59	56 (50–59)
(Chr. 7q21.3)	#18[a]	55	57	56	57	57	58	58	56	50	55 (50–59)
	#19	53	55	54	55	54	58	57	56	58	53 (48–59)
	#20	56	57	56	57	55	58	59	55	59	54.5 (50–59)
	#21[a]	51	55	51	55	52	54	54	51	54	50 (45–55)
MEST-DMR	#22[a]	67	62	69	58	63	68	58	66	60	60 (56–70)
(Chr. 7q32.2)	#23[a]	66	63	68	57	63	67	58	64	60	59 (55–69)
	#24	62	59	66	55	62	65	56	62	59	58 (52–68)
	#25	70	64	70	58	68	69	65	67	65	61 (42–73)
	#26[a]	61	59	65	55	63	64	57	61	57	57 (47–66)
	#27	68	62	72	60	67	67	60	70	61	60 (54–70)
H19-DMR	#28	51	41	51	49	48	50	41	52	58	48 (37–60)
(Chr. 11p15.5)	#29	50	45	51	50	48	52	42	53	58	50 (39–64)
	#30	48	40	49	48	46	49	39	50	57	46 (36–57)
	#31	44	40	49	41	46	48	39	49	49	45 (36–55)
Kv-DMR	#32	57	54	49	50	53	55	55	54	56	58 (49–66)
(Chr. 11p15.5)	#33	61	55	52	54	56	56	57	55	57	61 (52–68)
	#34	53	49	44	45	48	48	50	48	51	48 (41–54)
	#35	55	52	46	45	51	50	52	52	53	48 (42–55)
	#36	62	56	55	55	58	57	57	57	58	67 (55–72)
	#37	62	58	52	55	59	57	58	56	62	64 (55–71)

The hypomethylated and hypermethylated CpG sites are highlighted with light gray and dark gray backgrounds, respectively.

The values outside the normal ranges were confirmed by triplicate experiments. The mean value of the three experiments is shown.

[a]These 11 CpG sites have also been examined by array-based methylation analysis with HM450k.

DMR, differentially methylated regions.

Table 1 continued on next page

Table 1 Continued

		Temple syndrome				Kagami-Ogata syndrome					Controls (n=50)
DMR	**CpG**	**Pt. 1**	**Pt. 2**	**Pt. 3**	**Pt. 4**	**Pt. 5**	**Pt. 6**	**Pt. 7**	**Pt. 8**	**Pt. 9**	**Median (Min–Max)**
SNRPN-DMR	#38	40	41	39	45	40	43	37	39	40	42 (36–47)
(Chr. 15q11.2)	#39	41	41	38	45	42	41	39	39	40	43 (36–48)
	#40	42	42	40	46	43	44	39	39	43	44 (36–50)
	#41	42	42	39	46	46	44	41	39	41	44 (37–48)
	#42	38	38	36	39	36	38	36	35	37	38 (32–42)
	#43	42	42	40	43	41	41	40	39	41	42 (36–47)
GNAS-A/B-DMR	#44[a]	43	44	42	44	43	43	42	43	42	41 (34–45)
(Chr. 20q13.32)	#45[a]	43	44	41	44	44	43	42	43	41	40 (33–45)
	#46	44	46	45	47	47	46	44	47	44	43 (35–47)
	#47	41	42	40	42	41	40	40	41	40	38 (32–42)
	#48	41	42	40	42	44	42	42	44	42	40 (33–45)
	#49	39	40	39	40	42	40	40	39	38	38 (31–42)
	#50	41	43	41	44	44	42	43	44	41	40 (32–44)
Abnormally methylated DMRs in the HM450k analysis											
ZDBF2-DMR	#51	82	58	61	60	60	60	61	58	59	60 (58–68)
(Chr. 2q33.3)	#52	68	43	48	46	46	47	49	44	46	44 (40–49)
	#53	71	56	55	54	54	55	54	51	55	55 (47–62)
ZNF597-DMR	#54	34	60	66	63	60	67	64	60	61	59 (53–67)
(Chr. 16p13.3)	#55	32	55	66	65	57	66	62	58	58	58 (51–69)
	#56[a]	33	58	64	62	58	66	62	57	55	59 (51–68)
	#57	32	59	67	68	60	68	63	59	59	61 (50–69)
	#58	30	52	62	60	48	65	57	53	51	54 (41–67)
ZNF597/NAA60-DMR	#59	83	47	55	53	58	51	51	59	55	55 (43–60)
(Chr. 16p13.3)	#60[a]	86	42	52	52	57	50	51	56	55	53 (41–62)
	#61	74	40	48	47	54	47	45	53	52	48 (37–55)
	#62	87	55	59	55	60	53	56	58	59	58 (50–62)

The hypomethylated and hypermethylated CpG sites are highlighted with light gray and dark gray backgrounds, respectively.

The values outside the normal ranges were confirmed by triplicate experiments. The mean value of the three experiments is shown.

[a]These 11 CpG sites have also been examined by array-based methylation analysis with HM450k.

DMR, differentially methylated regions.

DISCUSSION

We performed genome-wide MLID analysis for four TS14 and five KOS14 patients with epimutations. MLIDs were found in Leu-gDNA and Buc-gDNA of patient 1 and in Leu-gDNA of patient 3 with TS14. In particular, the MLIDs identified in Leu-gDNA (the GOMs at *ZDBF2*-DMR and *ZNF597*/*NAA60*-DMR in patient 1 and the GOM at *GNAS-A*/*B*-DMR in patient 3) would be consistent with the expression data using immortalized lymphocytes. Indeed, under normal conditions, *ZDBF2* is expressed from a paternally derived chromosome with methylated *ZDBF2*-DMR,[11] *ZNF597* is expressed from a maternally inherited chromosome with unmethylated *ZNF597*/*NAA60*-DMR,[12] and *GNAS-A/B* is expressed from a paternally derived chromosome with unmethylated *GNAS-A*/*B*-DMR.[13] By contrast, because MLID was absent from KOS14 patients, the GOM at IG-DMR and *MEG3*-DMR may occur as an isolated epimutation.

Several findings are notable with regard to the identified MLIDs. First, the degrees of GOMs at *ZBDF2*-DMR and *ZNF597*/*NAA60*-DMR in patient 1 differed between Leu-gDNA and Buc-gDNA, and the LOM at *PPIEL*-DMR in patient 1 and GOM at *GNAS-A/B*-DMR in patient 3 were found only in Buc-gDNA and Leu-gDNA, respectively. The extents of LOMs at *MEG3*-DMR also differed between Buc-gDNA and Leu-gDNA of patients 3 and 4. These findings imply the occurrence of somatic mosaicism caused by defective maintenance of methylation patterns at these DMRs during development.[14] This notion assumes that the associated GOM-type dominant MLIDs in patients 1 and 3 with TS14 have taken place independently of the LOM-type epimutations at *MEG3*-DMR.

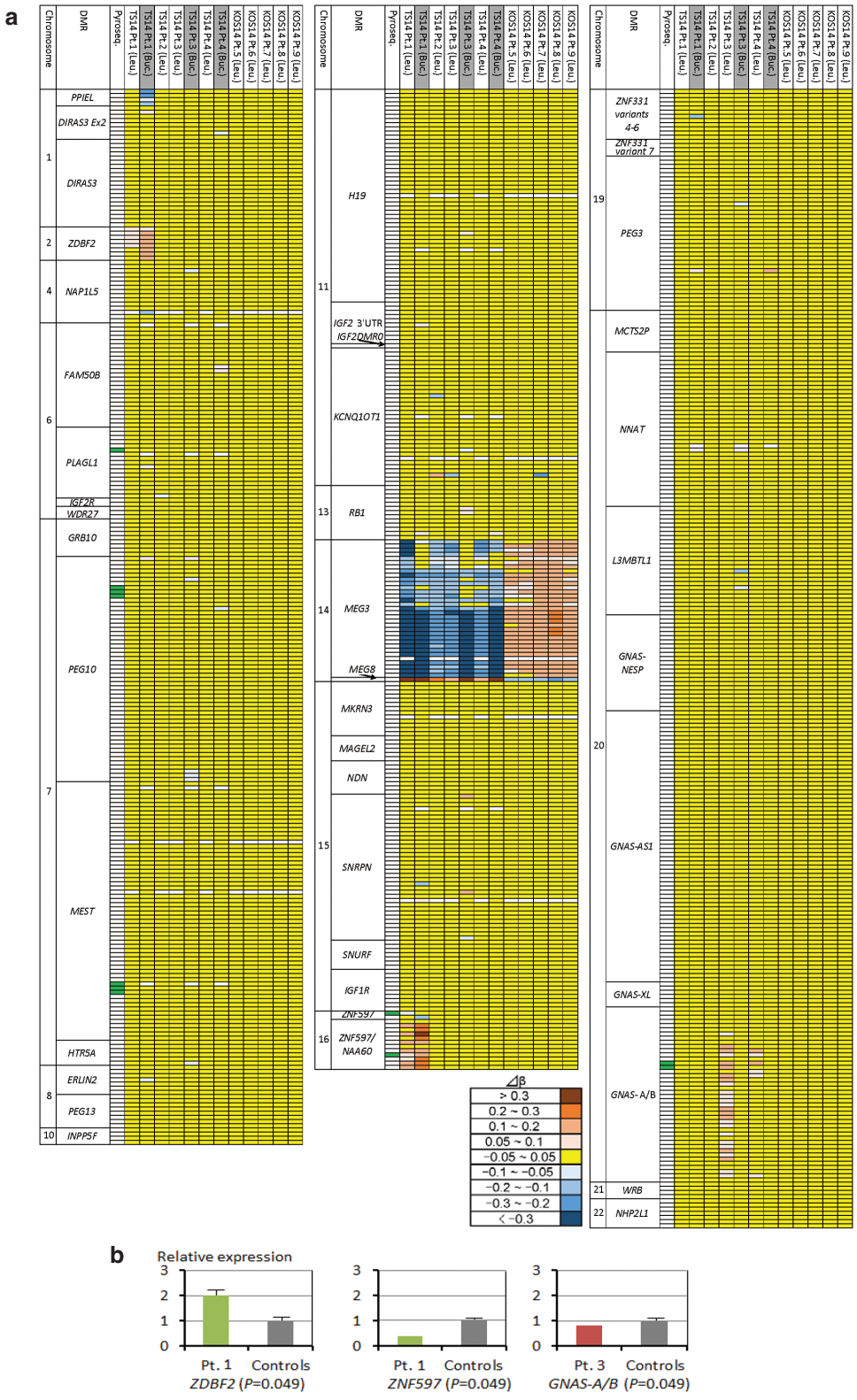

Figure 1 Methylation and expression analyses. (**a**) Heat map indicating the Δβ values for 753 probes (CpG sites) examined by HumanMethylation450 BeadChip using Leu-gDNA (Leu.) and Buc-gDNA (Buc.). The methylation levels of CpG sites are classified into nine categories based on Δβ values. The open rectangles indicate CpG sites with no signal intensities. A single row indicates a single probe (CpG site). Green rectangles represent 11 CpG sites that were also examined by pyrosequencing (Table 1). (**b**) Quantitative real-time polymerase chain reaction analysis using immortalized lymphocytes. Shown are relative mRNA expression levels for *ZDBF2*, *ZNF597*, and *GNAS-A/B* against *GAPDH* (mean ± SE). The expression studies were performed three times for each sample. Statistical significance between patients and controls was examined by the Mann-Whitney *U*-test.

Consistent with this, no pathologic mutation was identified in the six genes for MLIDs. However, the possibility of a mutation in a hitherto-unknown gene for MLIDs has not been excluded formally, and further studies are required to elucidate the underlying factors for the development of MLIDs. Second, GOM at *GNAS-A/B*-DMR in Leu-gDNA of patient 3 was identified by HM450k analysis but not by pyrosequencing analysis, with discordant results for the same #44 and #45 CpG sites (**Table 1**). This would be due primarily to the differences in the control subjects and the normal ranges (average ± 3 SD range for HM450k analysis as used in the previous study,[4] and the minimum–maximum range for pyrosequencing analysis as used in our previous study[10]) between the two analyses. Age-, sex-, and race-specific normal ranges would need to be established to permit data comparison among different studies and different methods. Finally, MLIDs in patient 1 were detected in ID-unrelated nonclassic DMRs. Recent array-based studies have also detected MLIDs in such DMRs.[5] Thus, application of array-based analysis in epimutation-positive patients, including those who have been studied by conventional methylation analyses only, would facilitate the identification of MLIDs affecting such DMRs.

Several additional matters are also worth pointing out. First, *MEG8*-DMR exhibited methylation patterns opposite to those of IG-DMR and *MEG3*-DMR, as previously reported.[15,16] This exemplifies the complexity of the methylation patterns of DMRs within a given imprinted region. Second, *GPR1-AS*-DMR was hypermethylated in Leu-gDNA of all patients and control subjects. Thus, although *GPR1-AS*-DMR remains a maternally methylated DMR and appears to control the methylation pattern of the paternally methylated secondary *ZDBF2*-DMR in the placenta,[11,15,17] it is unlikely that such an interaction underlies in the development of GOM at *ZDBF2*-DMR in Leu-gDNA and Buc-gDNA of patient 1. Third, LOM at *ZNF597*-DMR co-existed with GOM at *ZNF597*/*NAA60*-DMR in Leu-gDNA of patient 1. This is consistent with the maternally methylated *ZNF597*-DMR functioning as an upstream regulator for the methylation pattern of the secondary paternally methylated *ZNF597*/*NAA60*-DMR.[12,15]

Clinical features of patients 1 and 3 appear to be within the phenotypic spectrum of TS14, despite the presence of MLIDs. Indeed, TS14 patients have been identified primarily by PWS- or SRS-like phenotypes.[2] However, it is known that UPD(16)mat with GOM of *ZNF597*-DMR and excessive *ZNF597* expression is associated with pre- and postnatal growth failure,[18] as is UPD(20)mat with GOM at *GNAS-A/B*-DMR and no *GNAS-A/B* expression.[19] Thus, it may be possible that the LOM of *ZNF597*-DMR is relevant to the normal fetal growth in patient 1, and that the GOM at *GNAS-A/B* -DMR is involved in the growth failure in patient 3. In addition, because *ZDBF2* is expressed in the fetal mouse,[11] the GOM of *ZDBF2*-DMR also may have played a certain role in the growth pattern of patient 1. Furthermore, although it remains unknown why TS14 patients show PWS- or SRS-like features, more severe LOMs at *MEG3*-DMR in patient 1 than in patients 2–4 might be involved in the phenotypic difference. In addition, although the methylation patterns of the PWS- and SRS-related DMRs were normal in the examined tissues of patients 1–4, there might be abnormally methylated DMR(s) hidden in the critical tissues.[20]

In summary, we identified MLIDs in two of four patients with TS14 and none of five patients with KOS14 with epimutations. Further studies will permit a better assessment of the frequency of MLIDs and the phenotypic consequences of MLIDs in patients with IDs.

SUPPLEMENTARY MATERIAL

Supplementary material is linked to the online version of the paper at http://www.nature.com/gim

ACKNOWLEDGMENTS

We are grateful to all of the patients and their parents for their cooperation. We thank Toshiro Nagai, Rika Kosaki, Seiji Mizuno, Yasuhiro Naiki, Kenji Kurosawa, Goro Sasaki, Kouji Masumoto, Yumiko Komatsu, Akiko Yamamoto, and Takashi Imamura for providing us with clinical data and materials for molecular studies. We also thank Hiromi Kamura, Tamae Tanji, and Akihiro Umezawa for their support regarding molecular analyses. This work was supported by grants from the Japan Society for the Promotion of Science (JSPS) (A-25253023 and 15K15096), the National Center for Child Health and Development (25-10 and 28-6), the Japan Agency for Medical Research and Development (AMED) (16ek0109067h0003, 16ek0109030h0003, and 16ek0109141h0002), the Takeda Science Foundation, and the Daiichi Sankyo Foundation.

DISCLOSURE

The authors declare no conflict of interest.

REFERENCES

1. Ogata T, Kagami M. Kagami-Ogata syndrome: a clinically recognizable upd(14) pat and related disorder affecting the chromosome 14q32.2 imprinted region. *J Hum Genet* 2016;61:87–94.
2. Ioannides Y, Lokulo-Sodipe K, Mackay DJ, Davies JH, Temple IK. Temple syndrome: improving the recognition of an underdiagnosed chromosome 14 imprinting disorder: an analysis of 51 published cases. *J Med Genet* 2014;51:495–501.
3. Mackay DJ, Eggermann T, Buiting K, et al. Multilocus methylation defects in imprinting disorders. *Biomol Concepts* 2015;6:47–57.
4. Court F, Martin-Trujillo A, Romanelli V, et al. Genome-wide allelic methylation analysis reveals disease-specific susceptibility to multiple methylation defects in imprinting syndromes. *Hum Mutat* 2013;34:595–602.
5. Docherty LE, Rezwan FI, Poole RL, et al. Mutations in NLRP5 are associated with reproductive wastage and multilocus imprinting disorders in humans. *Nat Commun* 2015;6:8086.
6. Rosenfeld JA, Fox JE, Descartes M, et al. Clinical features associated with copy number variations of the 14q32 imprinted gene cluster. *Am J Med Genet A* 2015;167A:345–353.
7. Corsello G, Salzano E, Vecchio D, et al. Paternal uniparental disomy chromosome 14-like syndrome due a maternal de novo 160 kb deletion at the 14q32.2 region not encompassing the IG- and the MEG3-DMRs: Patient report and genotype-phenotype correlation. *Am J Med Genet A* 2015;167A:3130–3138.
8. Briggs TA, Lokulo-Sodipe K, Chandler KE, Mackay DJ, Temple IK. Temple syndrome as a result of isolated hypomethylation of the 14q32 imprinted DLK1/MEG3 region. *Am J Med Genet A* 2016;170A:170–175.

9. Sachwitz J, Strobl-Wildemann G, Fekete G, et al. Examinations of maternal uniparental disomy and epimutations for chromosomes 6, 14, 16 and 20 in Silver-Russell syndrome-like phenotypes. *BMC Med Genet* 2016;17:20.
10. Kagami M, Mizuno S, Matsubara K, et al. Epimutations of the IG-DMR and the MEG3-DMR at the 14q32.2 imprinted region in two patients with Silver-Russell Syndrome-compatible phenotype. *Eur J Hum Genet* 2015;23:1062–1067.
11. Kobayashi H, Yamada K, Morita S, et al. Identification of the mouse paternally expressed imprinted gene Zdbf2 on chromosome 1 and its imprinted human homolog ZDBF2 on chromosome 2. *Genomics* 2009;93:461–472.
12. Nakabayashi K, Trujillo AM, Tayama C, et al. Methylation screening of reciprocal genome-wide UPDs identifies novel human-specific imprinted genes. *Hum Mol Genet* 2011;20:3188–3197.
13. Maupetit-Méhouas S, Azzi S, Steunou V, et al. Simultaneous hyper- and hypomethylation at imprinted loci in a subset of patients with GNAS epimutations underlies a complex and different mechanism of multilocus methylation defect in pseudohypoparathyroidism type 1b. *Hum Mutat* 2013;34:1172–1180.
14. Azzi S, Blaise A, Steunou V, et al. Complex tissue-specific epigenotypes in Russell-Silver Syndrome associated with 11p15 ICR1 hypomethylation. *Hum Mutat* 2014;35:1211–1220.
15. Court F, Tayama C, Romanelli V, et al. Genome-wide parent-of-origin DNA methylation analysis reveals the intricacies of human imprinting and suggests a germline methylation-independent mechanism of establishment. *Genome Res* 2014;24:554–569.
16. Bens S, Kolarova J, Gillessen-Kaesbach G, et al. The differentially methylated region of MEG8 is hypermethylated in patients with Temple syndrome. *Epigenomics* 2015;7:1089–1097.
17. Sanchez-Delgado M, Martin-Trujillo A, Tayama C, et al. Absence of maternal methylation in biparental hydatidiform moles from women with NLRP7 maternal-effect mutations reveals widespread placenta-specific imprinting. *PLoS Genet* 2015;11:e1005644.
18. Azzi S, Salem J, Thibaud N, et al. A prospective study validating a clinical scoring system and demonstrating phenotypical-genotypical correlations in Silver-Russell syndrome. *J Med Genet* 2015;52:446–453.
19. Mulchandani S, Bhoj EJ, Luo M, et al. Maternal uniparental disomy of chromosome 20: a novel imprinting disorder of growth failure. *Genet Med* 2016;18:309–315.
20. Alders M, Maas SM, Kadouch DJ, et al. Methylation analysis in tongue tissue of BWS patients identifies the (EPI)genetic cause in 3 patients with normal methylation levels in blood. *Eur J Med Genet* 2014;57:293–297.